AIAA JOURNAL
Vol. 47, No. 3, March 2009

Interval-Based Multi-Objective Optimization of Aircraft Wings Under Gust Loads

Luna Majumder* and S. S. Rao†
University of Miami, Coral Gables, Florida 33124-0624

DOI: 10.2514/1.37224

An interval-based modified game theory approach is presented for the multi-objective optimization of aircraft wing structures by including the effect of uncertainty present in the atmospheric turbulence. The methodology is illustrated with two examples: a symmetric double-wedge airfoil, based on a beam-type analysis, and a supersonic airplane wing, based on a finite element analysis. The design parameters of the aircraft wing are assumed to be uncertain and are described by a range of values. Because the interval ranges of response parameters are found to increase with an increase in the number and/or ranges of input interval parameters, a truncation procedure is used to obtain an approximate but reasonably accurate response of the structure. An interval-based game theory technique, coupled with interval-based nonlinear programming techniques, is used for the optimum solution of the two aircraft wings considered. The present methodology is expected to be useful in all practical situations with conflicting goals/objectives, and where the ranges of the uncertain parameters are readily available, whereas information on the probability distributions or evidence data of the uncertain design variables may not be easily available.

Nomenclature

$[A]$, $[B]$, $[C]$, $[D]$	=	component matrices used in defining the aerodynamics matrix $[Q]$
A_j	=	area of jth plate element
$\mathbf{a}$	=	vector of interpolation functions
a_∞	=	freestream speed of sound
b_r	=	some reference length
D	=	total drag
E	=	Young's modulus
F_g	=	force applied to tire by ground
$f(\mathbf{X})$	=	objective function
i	=	number of constraints
K	=	stiffness matrix in flutter analysis
$[K]$	=	stiffness matrix for flutter analysis
k_r	=	reduced frequency
$[M]$	=	mass matrix for flutter analysis
M_F	=	flutter Mach number
M_∞	=	flight Mach number
n	=	number of design variables
P_i	=	ith generalized force
p_∞	=	freestream pressure of air
$[Q]$	=	air-force matrix used in flutter analysis
V, V_∞	=	freestream velocity $= a_\infty M_\infty$
V_F	=	flutter velocity
$\mathbf{X}$	=	vector of design variables
x_j	=	jth design variable
$x_j^{(l)}$	=	lower bound on jth design variable
$x_j^{(u)}$	=	upper bound on jth design variable
$\boldsymbol{\xi}$	=	vector of modal participation coefficients
ξ_i	=	ith generalized coordinate
ρ_∞	=	density of air
σ_g	=	maximum gust-induced stress
τ_f	=	duration of flight
υ	=	Poisson's ratio
ω_F	=	flutter frequency

Received 19 February 2008; revision received 29 August 2008; accepted for publication 15 October 2008.

*Graduate Student, Department of Mechanical and Aerospace Engineering; currently Research Structural Engineer, Permasteelisa North America Corporation, 7933 NW 71st Street, Miami, FL 33166.

†Professor and Chairman, Department of Mechanical and Aerospace Engineering. Associate Fellow AIAA.

Introduction

IN MOST real-world problems, several goals must be satisfied simultaneously to obtain an optimal solution. The multiple objectives are typically conflicting and noncommensurable and must be satisfied simultaneously. For example, in the design of an aircraft wing, the simultaneous minimization of weight and maximization of flutter velocity might be necessary. If weight is reduced (improved), the flutter velocity becomes smaller (worse). This is a multi-objective problem with two opposing objectives, where a step toward improving one of the objectives indicates a step away from improving the other. The earliest reported in-depth work on the formulation of a multi-objective problem is that of Kuhn and Tucker [1]. Since then several techniques have been suggested by researchers for the solution of a multi-objective optimization problem.

A common approach is the combination of all the objectives into a single-objective function using a weighted sum method [2]. Thus if $f_1(X)$ and $f_2(X)$ denote two objective functions, construct a new objective function for optimization as $f(X) = \alpha_1 f_1(X) + \alpha_2 f_2(X)$, where α_1 and α_2 denote the weight of one objective function relative to the other. This weighting approach is based on the assumption that the objective functions are mutually independent. This technique has the drawback of modeling the original problem in an inadequate manner, generating solutions that will require further sensitivity analysis before becoming reasonably useful to the designer. This method is also incapable of generating the entire set of Pareto optimal solutions for nonconvex problems. Another approach is to choose one objective and incorporate the other objective(s) as constraints. This approach has the disadvantage of limiting the choices available to the designer, making the optimization process a rather difficult task. The two-level game theory approach presented by Rao et al. [3] overcomes some of the shortcomings of the weighting method but this method is computationally very expensive. Osman et al. in 2004 [4] proposed a three-level nonlinear multi-objective decision-making problem with linear or nonlinear constraints in which the objective functions at every level are nonlinear functions which are to be maximized.

Recent advances in structural optimization have resulted in the development of techniques for handling problems involving different types of uncertainty. Rao [5] presented a method for solving fuzzy multi-objective optimization problems using ordinary nonlinear programming techniques. Rao et al. [6] proposed two procedures, namely, the λ formulation and the α-cut approach for solving multi-objective optimization. λ formulation provides an overall compromise solution whereas the α-cut approach yields the design information in a parametric form. Yu and Xu [7] have presented three approaches by using different types of generalized fuzzy decision making: intersection decision, convex decision, and product decision in order to reflect various decision ideas and provide the favorable condition for the selection of structural design schemes. The game theory approach [8–12] has been found to be superior to many other techniques because it finds not only the best compromise (Pareto optimal) solution but also the relative contributions of the various objective functions to the best compromise solution.

This paper deals with an interval-based game theory approach for multi-objective optimum design of wing structures subjected to constraint due to gust loads as one of the primary behavior constraints. An interval analysis-based truncation technique [13] is used to avoid unnecessary growth of response quantities. For comparison purposes, the multi-objective optimization problem is also solved using deterministic and probabilistic approaches.

Interval Analysis

Interval Approach

Quite often, however, the amount of information available on the uncertain parameters is not enough to accurately define the probability distribution functions. Even small deviations from the real distributions may cause large errors in the value of the probability of being in the feasible region of the domain space and then to unreliable results of the optimization. In fact, in the design problems there exist a vast amount of fuzzy information. If the structural parameters are assumed to be interval variables, then the objective function and the constraint conditions of the optimization problem are intervals. For example, the stress induced in a structure may be constrained by an upper bound value as $s \leq s^u$; this implied that $s = s^u$ is acceptable but $s = s^u + \Delta s$ is unacceptable, even for a very small value of Δs. It is more acceptable to assign a transition stage from absolute acceptance to absolute unacceptance. At the same time, the design load P of structures may be constrained by a lower bound value as $P \geq P^l$; in other words, $P = P^l$ is acceptable but $P = P^l - \Delta P$ is unacceptable, even for a very small value of ΔP.

Concept of Interval Value

An interval parameter represents the range of variation of an uncertain variable. For each imprecise parameter, there are two numbers that represent its lower and upper bounds. Because it is not always possible to find the detailed information on the uncertainty of a parameter, an interval statement can be conveniently used as a general indication of the imprecision that exists in most engineering design problems. This means that we need not know the probability distributions of the random variables or the fuzzy subsets of the uncertain variables. In this work, all the system parameters are treated as interval numbers as $A = [A - \Delta A, A + \Delta A]$ with A denoting the nominal or mean value and ΔA the deviation from the mean on either side. For example, in a structural system, the geometry parameter of a component, such as the cross-sectional area of a beam, can be taken as an interval value because of the manufacturing tolerance, $\pm\Delta A$. Similarly, the load applied to a structure P is usually known to vary between the values $\underline{P}$ and $\bar{P}$, with no information on its probability distribution and hence it can be expressed by the interval $[\underline{P}, \quad \bar{P}]$, where $\underline{P}$ is the minimum value and $\bar{P}$ is the maximum value of the load. The interval analysis involves the application of interval arithmetic to every step of the calculations.

Necessity of Truncation Method

For the development of the interval analysis procedure involving large systems of linear equations, different approaches have been investigated and the numerical solutions given by the various methods have been compared with each other. The field of interval analysis, as applied to engineering, has been presented by Rao and Berke [13]. It is found that the traditional combinatorial method is only suitable to problems with a limited number of interval variables. Otherwise, it will become a tedious and expensive procedure. Other approaches, such as the direct implementation of the Gaussian elimination method and the inequality-based method, have the tendency of overestimating the solution, especially when the input parameters have wide ranges of uncertainty. Although these methods have the advantage of being applicable for achieving a conservative design, the results are not always accurate enough.

In comparison, the truncation method presented in [13] can yield reasonable solutions even when the widths of their starting points or the interval ranges of other influencing parameters are quite large. In complicated problems where there are a large number of interval operations in each expression, a specific interval may appear several times in different terms of the same equation causing the width of the response parameter wider than the true width. This means that the exact range of the function cannot be computed. Thus, with an increasing number of interval variables involved in the calculation and arithmetic operations performed in between, the width of the interval of the solution definitely increases. To limit the growth of intervals of response parameters for large amounts of uncertainty, the interval-truncation method can be used based on a comparison of the input and output ranges of the parameters and computed responses.

Truncation Procedure

Let two interval values $a = [\underline{a}, \quad \bar{a}]$ and $b = [\underline{b}, \quad \bar{b}]$ be used to find the computed output $c = [\underline{c}, \quad \bar{c}]$. If we use the central values of the variables $a_o = (\underline{a} + \bar{a})/2$ and $b_o = (\underline{b} + \bar{b})/2$ to do the same (crisp) calculation, we get the output c_o. Then we use c_o to judge the necessity of applying truncation. Let $\varepsilon = 10^{-5}$ represent a very small number. Then we try to obtain the refined results as $c \approx [\underline{d}, \quad \bar{d}]$. If c_o is close to zero, no truncation needs to be used:

$$\underline{d} = \underline{c}; \qquad \bar{d} = \bar{c}, \quad \text{if } c_o \leq \varepsilon \tag{1}$$

Otherwise, the truncation method is implemented as follows (Fig. 1):

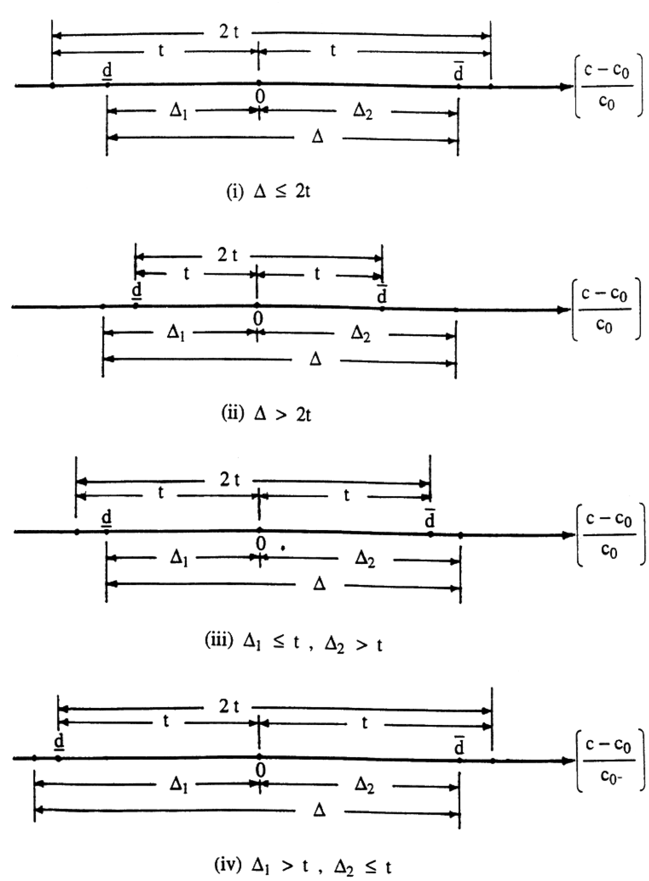

Fig. 1 Interval analysis (truncation method).

1) Find the relative deviation (Δ) of the interval range ($\bar{c} - \underline{c}$) as

$$\Delta_1 = \left|\frac{c_o - \underline{c}}{c_o}\right|; \qquad \Delta_2 = \left|\frac{\bar{c} - c_o}{c_o}\right|; \qquad \Delta = \Delta_1 + \Delta_2 = \bar{c} - \underline{c} \tag{2}$$

2) Because the deviation (Δ) should be larger or equal to the exact deviation, we specify the maximum permissible range of ($\bar{c} - \underline{c}$) to be equal to $2t$. t can be selected to be equal to the maximum of the relative deviations of the input variables a and b from their respective central values:

$$t = \max\left(\left|\frac{\bar{a} - \underline{a}}{a_o}\right|, \left|\frac{\bar{b} - \underline{b}}{b_o}\right|\right) \tag{3}$$

3) Use t to compare the deviations and the range of c is truncated according to the following scheme:

$$\begin{array}{ll} \underline{d} = \underline{c}; \quad \bar{d} = \bar{c}, & \text{if } \Delta_1 \le t \text{ and } \Delta_2 \le t \\ \underline{d} = c_o + t(\underline{c} - c_o); \quad \underline{d} = \underline{c}, & \text{if } \Delta_1 > t \text{ and } \Delta_2 \le t \\ \underline{d} = \underline{c}; \quad \bar{d} = c_o + t(\bar{c} - c_o), & \text{if } \Delta_1 \le t \text{ and } \Delta_2 > t \\ \underline{d} = c_o + t(\underline{c} - c_o); \quad \bar{d} = c_o + t(\bar{c} - c_o), & \text{if } \Delta_1 > t \text{ and } \Delta_2 > t \end{array} \tag{4}$$

In numerical experiments, compared to the combinatorial method, the truncation method is found to be fast and reasonably accurate.

Interval Solution of Finite Element Equations

To understand the dynamic behavior of any practical structure or machine, the finite element modeling is necessary, which leads to a linear system of equations. If some of the structural or mechanical parameters are uncertain at the design stage, the matrices given by the finite element theory are interval matrices, and the problem is generally written as

$$[K]\{x\} = \{b\} \tag{5}$$

with $[K] \in$ [K] and $\{b\} \in$ {b}. Several algorithms intend to solve this problem, but they lead to an overestimation of the solution. A method based on Rump's iterative technique, developed by Dessombz et al. [14], is used in this work for solving such problems. It is an iterative method relying on a fixed point theorem that leads to a sharp result quite fast. For a structural or mechanical problem, the stiffness matrix and the load vector are written with a factorized parameter as

$$[\mathrm{K}] = [K_O] + \alpha[K_1] \tag{6}$$

and

$$\{\mathrm{b}\} = \{b_O\} + \beta\{b_1\} \tag{7}$$

with α and β as the independent centered intervals, generally $[-1, 1]$. $[K_O]$ and $\{b_O\}$ correspond to the matrix and the vector built from the mean values of the parameters. The $[K]$ matrix remains symmetric positive definite for each value of ε_n due to the physical nature of the parameters. This method is based on the fixed point theorem and avoids the problems of overestimation due to the loss of dependence in interval arithmetic. The algorithm can be implemented as follows: Consider a system in which only one parameter is an interval, and then

$$[A] = [A_O] + \alpha[A_1] \tag{8}$$

where α is centered denotes the equation of the system.

Initialization stage:

$$\varepsilon = [\,0.9 \quad 1.1\,]$$

is the inflation parameter;

$$[R] = \mathrm{inv}(\mathrm{mid}[\mathrm{A}]) = [A_O]^{-1}$$

is an estimation of the inverse of mid[A];

$$\{x_s\} = [R] * \{b\}$$

is an estimation of the solution;

$$[B] = [A_O]^{-1}[A_1]$$

$$\{g\} = [R] * (\{b\} - [A] * \{x_s\}) = -\alpha[A_O]^{-1}[A_1][A_O]\{b\} = -\alpha[B]\{x_s\}$$

$\{x_O\} = \{g\}$ is the initialization of the solution $\{x^*\}$;

$$[G] = [I] - [R] * [A] = -\alpha[B]$$

is the iteration matrix in the equation

$$\{x^*\} = [G]\{x^*\} + \{g\} \tag{9}$$

Iterative resolution:

$$\{y\} = \varepsilon * \{x\}; \qquad \{x\} = \{g\} + [G] * \{y\}$$

until $\{x\} \subset \{y^O\}$ or too many iterations. If the condition $\{x\} \subset \{y^O\}$ is satisfied, then $\{x\}$ is a conservative solution of the equation $[A]\{x\} = \{b\}$.

It must be noted that all the matrix multiplications and linear system resolutions involve only deterministic matrices (as opposed to interval ones). The interval formulation is preserved, and the interval parameters are put into factors in front of deterministic matrices. The control of the intervals is essential to avoid large overestimations of the solutions.

Gust Analysis

Stress Induced in the Wing due to Gust

Two basic approaches are generally used for the structural design of an aircraft under a gust encounter. The first approach is based on the assumption of a discrete gust, and the second approach is based on a random gust described by power spectral techniques. In the discrete gust approach, the gust is considered to be a one-minus-cosine type and uniform along the span of the wing. In the power spectral technique, the vertical velocity due to gust is treated as a stochastic process for the computation of the gust-induced stresses. Methods of discrete gust design were described in detail by Philip [15]. In recent years, airplane designs have usually incorporated both the single-gust concept and the concept of a random gust, frequently represented by a statistical model. The methods of deterministic and probabilistic gust analysis have been done by several researchers [16–24].

Discrete Gust

To find the stresses developed in a wing due to a discrete gust, the equations of motion of the aircraft are formulated with the vertical motion and wing bending modes as generalized coordinates. The gust is considered sinusoidal and uniform along the span of the wing. The transverse displacement of the middle surface of the wing can be expressed as

$$w(y,t) = \sum_{i=0}^{n} w_i(y)\xi_i(t) \tag{10}$$

and the equations of motion in terms of the generalized coordinates, $\xi_i(t)$, as

$$M_i\ddot{\xi}_i(t) + \omega_i^2 M_i \xi_i(t) = P_i(t) \tag{11}$$

The generalized force in the ith mode P_i is given by

$$P_i(t) = \int_{-\frac{b}{2}}^{\frac{b}{2}} F(y,t) w_i(y)\,\mathrm{d}y \tag{12}$$

with

$$F = L_v + L_g = -\frac{a}{2}\rho c V \int_0^t \ddot{w}[1-\phi(t-\tau)]\,\mathrm{d}\tau + \frac{a}{2}\rho c V \int_0^t \dot{u}\psi(t-\tau)\,\mathrm{d}\tau \tag{13}$$

where $t = 0$ is the time from the start of gust penetration, a is the lift–curve slope, ρ is the density of air, c is the chord of the wing, V is the forward velocity of flight, u is the vertical velocity of the gust, $\{1-\phi(t)\}$ is the Wagner function which denotes the growth of lift on a wing following a sudden change in the angle of attack, and $\varphi(t)$ is the Küssner function which denotes the growth of lift on a rigid wing penetrating a sharp-edged gust. For two-dimensional incompressible flow, the functions $\{1-\phi(t)\}$ and $\varphi(t)$ are given by the approximations [25]

$$1-\phi(t) = 1 - 0.165e^{-0.09(\frac{V}{C})t} - 0.335e^{-0.6(\frac{V}{C})t} \tag{14}$$

and

$$\psi(t) = 1 - 0.5e^{-0.26(\frac{V}{C})t} - 0.5e^{-2(\frac{V}{C})t} \tag{15}$$

Figure 2 shows the plots of Wagner and Küssner functions which are calculated from Eqs. (14) and (15). Because only 2 degrees of freedom (vertical motion and fundamental wing bending) are sufficient to accurately predict the response, by substituting Eq. (10) into Eq. (13) and the resulting equation of F into Eq. (11), the following two response equations result with $i = 0$ and 1, respectively [25],

$$\frac{2M_O}{a\rho VS}\ddot{\xi}_O = -\int_o^t\left(\ddot{\xi}_O + \frac{S_1}{S}\ddot{\xi}_1\right)\{1-\phi(t-\tau)\}\,\mathrm{d}\tau + \int_o^t \dot{u}\psi(t-\tau)\,\mathrm{d}\tau \tag{16}$$

$$\frac{2M_1}{a\rho VS}\ddot{\xi}_1 + \frac{2\omega_1^2 M_1}{a\rho VS}\xi_1 = -\int_o^t\left(\frac{S_1}{S}\ddot{\xi}_O + \frac{S_2}{S}\ddot{\xi}_1\right)\{1-\phi(t-\tau)\}\,\mathrm{d}\tau + \frac{S_1}{S}\int_o^t \dot{u}\psi(t-\tau)\,\mathrm{d}\tau \tag{17}$$

where, because of symmetry of mode

$$S = 2\int_0^{\frac{b}{2}} c\,\mathrm{d}y, \qquad S_1 = 2\int_0^{\frac{b}{2}} c w_1(y)\,\mathrm{d}y$$

$$S_2 = 2\int_0^{\frac{b}{2}} c w_1^2(y)\,\mathrm{d}y$$

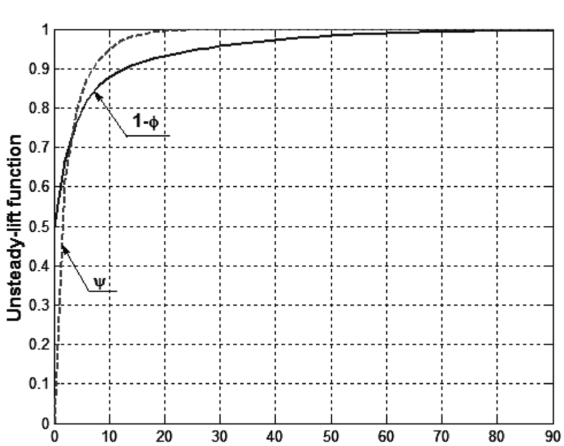

Fig. 2 Unsteady-lift functions; where for a sharp-edge gust, the gust force is $f(s) = \psi(s)$.

$$M_o = 2\int_{-\frac{b}{2}}^{\frac{b}{2}} m w_o^2\,\mathrm{d}y$$

and

$$M_1 = 2\int_{-\frac{b}{2}}^{\frac{b}{2}} m w_1^2\,\mathrm{d}y$$

By introducing nondimensional parameters s, σ, and z_1 as

$$s = 2V\frac{t}{c_o}, \qquad \sigma = 2V\frac{\tau}{c_o}, \qquad z_i = \frac{V}{Uc_o}\xi_i$$

with ($i = 0, 1$) Eqs. (16) and (17) can be written as

$$\mu_o z_o'' = -2\int_0^s (z_o'' + r_1 z_1'')[1-\phi(s-\sigma)]\,\mathrm{d}\sigma + \int_0^s \frac{u'}{U}\psi(s-\sigma)\,\mathrm{d}\sigma \tag{18}$$

and

$$\mu_o z_1'' + \mu_1\lambda^2 z_1 = -2\int_0^s (r_1 z_o'' + r_2 z_1'')[1-\phi(s-\sigma)]\,\mathrm{d}\sigma + r_1\int_0^s \frac{u'}{U}\psi(s-\sigma)\,\mathrm{d}\sigma \tag{19}$$

where

$$\mu_i = \frac{8M_i}{a\rho c_o S} \quad (i = 0, 1) \tag{20}$$

$$\lambda = \frac{\omega_1 c_o}{2V} \tag{21}$$

$$r_i = \frac{S_i}{S} \quad (i = 1, 2) \tag{22}$$

and a prime denotes a derivative with respect to σ. Here, μ_o and μ_1 are the mass parameters associated with vertical free-body motion of the airplane and with the fundamental mode, and λ is the reduced frequency. Equations (18) and (19) are the basic response equations in the gust analysis. The parameters appearing in Eqs. (20–22) depend upon the forward velocity, air density, lift–curve slope, and the airplane-physical characteristics: the wing planform, wing bending stiffness, and wing mass distribution. It can be seen from Eqs. (18) and (19) that if any one of the three quantities z_o, z_1, and u is known, the other two may be determined. Thus, if the gust is known, the response may be determined or conversely, if either z_o or z_1 is known, the gust may be determined. A useful equation relating z_o and z_1 may be found by combining Eqs. (18) and (19) so as to eliminate the integral dealing with the gust. Thus, the two simultaneous integro-differential equations (18) and (19) can be expressed in an equivalent form, as

$$\mu_o\alpha = -2\int_0^s (\alpha + r_1\beta)\theta(s-\sigma)\,\mathrm{d}\sigma + f(s) \tag{23}$$

and

$$\frac{\mu_1}{r_1}(\beta + \lambda^2 z_1) + 2\left(\frac{r_2}{r_1} - r_1\right)\int_0^s \beta\theta(s-\sigma)\,\mathrm{d}\sigma = \mu_o\alpha \tag{24}$$

where

$$\alpha = z_o'', \qquad \beta = z_1'', \qquad \theta = 1-\phi, \qquad f = \int_0^s \frac{u'}{U}\psi(s-\sigma)\,\mathrm{d}\sigma$$

to find $z_o(s)$ and $z_1(s)$.

These equations of motion are solved for the generalized coordinates $\xi_o(\tau)$ and $\xi_1(\tau)$ at the discrete time stations $\tau = 0$, $\Delta\tau$, $2\Delta\tau, \ldots$, by using the numerical procedure outlined in [26]. Here it is assumed that the airplane is in level flight before encountering the gust. The variation of the vertical gust velocity with time is assumed to be a one-minus-cosine type. Once the generalized coordinates $\xi_o(\tau)$ and $\xi_1(\tau)$ are known, the transverse displacement $w(x, y, \tau)$, the stresses induced and hence σ_g, the maximum gust stress induced at the root of the wing, can be computed from the standard theories of solid mechanics.

Random Gust: Power Spectral Approach

The discrete gust approach works well for gusts which are isolated or which are of a continuous-sinusoidal type. But this approach is not very reliable because it is difficult to establish the time history of any long gust sequence. So, to determine the effects of atmospheric turbulence on the dynamic response of an airplane, the atmospheric turbulence is considered as a random continuous turbulence. The vertical velocity due to gust is treated as a stochastic process for the computation of gust-induced stresses. By modeling the atmospheric turbulence as a stationary random process, the power spectral methods are used for finding the rms (root mean square) values of the stresses induced in the airplane wing structure as follows: If $u(t)$ represents a random disturbance or a system response quantity of this disturbance (such as atmospheric gust's vertical velocity and the resulting response), then the power-spectral-density (PSD) function $\phi(\omega)$ is defined as

$$\phi(\omega) = \lim_{T\to\infty} \frac{1}{2\pi T} \left| \int_{-T}^{T} u(t) e^{-\iota\omega t}\, \mathrm{d}t \right|^2 \tag{25}$$

where ω is the frequency (in rad/s), and the vertical bars designate the modulus of the complex quantity

$$\int_{-T}^{T} u(t) e^{-\iota\omega t}\, \mathrm{d}t$$

that represents the Fourier transform of $u(t)$. An equivalent and more useful expression for $\phi(\omega)$ can be derived as

$$\phi(\omega) = \frac{2}{\pi} \int_{-T}^{T} R(\tau) \cos\omega\tau \, \mathrm{d}\tau \tag{26}$$

where $R(\tau)$ is the autocorrelation function defined by

$$R(\tau) = \lim_{T\to\infty} \frac{1}{2\pi T} \int_{-T}^{T} u(t) u(t+\tau)\, \mathrm{d}t \tag{27}$$

A useful property of $\phi(\omega)$ is that

$$\int_0^{\infty} \phi(\omega)\mathrm{d}\omega = \text{mean square} = \overline{u^2(t)} = R(0) = \sigma^2 \tag{28}$$

The quantity $\overline{u^2(t)}$ or σ^2 is the time mean square. For a linear system, the relation between the spectrum of a disturbance or input $\phi_i(\omega)$ and the spectrum of the system response or output $\phi_0(\omega)$ is given by

$$\phi_o(\omega) = \phi_i(\omega)|H(\omega)|^2 \tag{29}$$

where $|H(\omega)|$ is the frequency response function for each frequency ω, which is defined as the system response to a sinusoidal disturbance of frequency ω and hence the spectrum of the response is computed by finding the stress response at a point in the airplane wing due to a unit sinusoidal gust. Because this sinusoidal gust can be treated as discrete, the deterministic gust analysis procedure described in the previous section can be used to find the transfer function $|H(\omega)|$. Thus, it becomes necessary to use the deterministic gust stress analysis a number of times in one probabilistic stress analysis. In Eq. (29), the turbulence is assumed as one dimensional which implies that at any instant of time, the vertical gust velocity is constant along the wing span or the scale of turbulence of the area under the correlation curve is large compared with the span of the wing. In this work, the spectrum of the vertical gust velocity is taken as

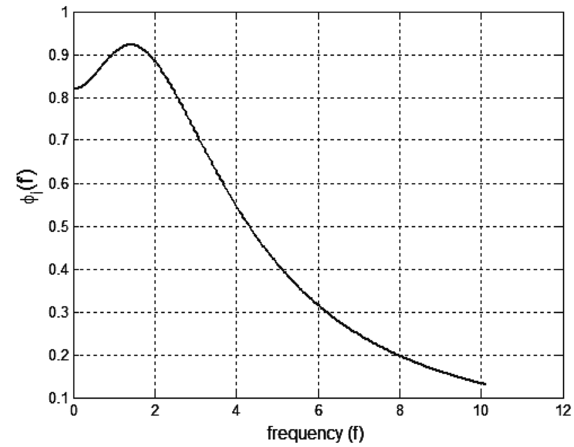

Fig. 3 Input PSD for random continuous turbulence ($f = \omega/2\pi$).

$$\phi_i(\omega) = \frac{2L}{V_g} \left\{ \frac{1 + (3L^2\omega^2/V_g^2)}{[1 + (L^2\omega^2/V_g^2)]^2} \right\} S_i^2 \tag{30}$$

L is the scale of turbulence, V_g is the forward velocity of flight at the instant of a gust encounter, and ω is the frequency. Figure 3 shows the PSD of the vertical gust velocity. Here, S_i is the rms value of the gust velocity given by

$$S_i^2 = \int_{-\infty}^{\infty} \phi_i(\omega)\, \mathrm{d}\omega \tag{31}$$

The spectrum of the response can be used to determine the rms value of the response S_o as

$$S_o^2 = \int_{-\infty}^{\infty} \phi_o(\omega)\, \mathrm{d}\omega \tag{32}$$

Interval Approach

It is known that the probabilistic approach cannot yield reliable results at required precision without sufficient experimental data to validate the joint probability densities of the random variables or functions involved. Further, the determination of the power-spectral-density functions of atmospheric turbulence for a wide range of atmospheric conditions is difficult. In the interval parameter-based optimum design, on the other hand, only the known or expected ranges of the parameters are required. So, if the parameters of a system are denoted by simple ranges, the interval analysis method described earlier can be used for the analysis of the system.

Optimization Problem

Problem Statement

The multi-objective optimization of two example wings is considered for illustration. The first example deals with the determination of the thickness T and chord length C of a hollow

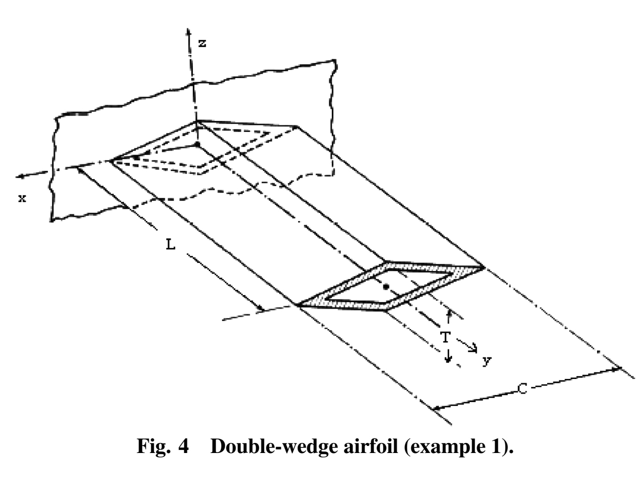

Fig. 4 Double-wedge airfoil (example 1).

symmetric double-wedge airfoil shown in Fig. 4 [27]. The minimizations of structural weight and energy required and the maximization of flutter speed are considered as the three objectives. The maximum stresses developed during gust (σ_g) are restricted and bounds are placed on the design variables. Thus the optimization problem becomes as follows: Find $\mathbf{X} = \{x_1, x_2\} = \{T, C\}$ which minimizes $f_1(\mathbf{X})$ and $f_2(\mathbf{X})$, and maximizes $f_3(\mathbf{X})$ subject to

$$\sigma_g(\mathbf{X}) \leq \sigma_g^{(u)} \tag{33}$$

$$x_i^{(l)} \leq x_i \leq x_i^{(u)}, \qquad i = 1, 2 \tag{34}$$

The weight of the airfoil given by

$$f_1(\mathbf{X}) = \tfrac{1}{2}\rho l \rho_s x_1 x_2 \tag{35}$$

and the energy required by

$$f_2(\mathbf{X}) = D(\mathbf{X}) V T_f \tag{36}$$

and $f_3(\mathbf{X})$ represents the flutter Mach number which can be calculated as indicated in the Appendix. In Eq. (36), D is the total drag which can be computed from the known flight conditions of the airfoil as

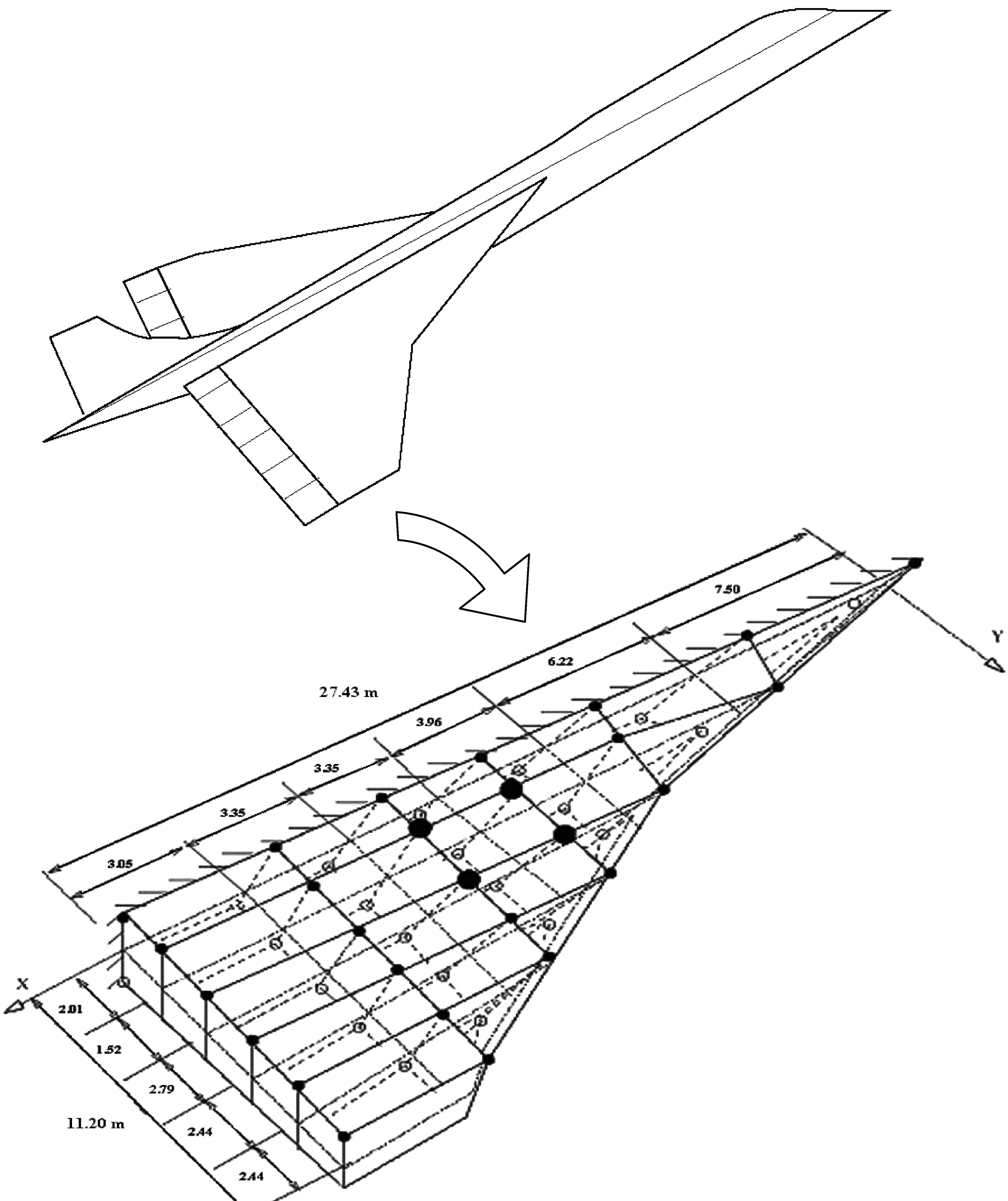

Fig. 5 Supersonic transport wing, finite element idealization (example 2).

$$D = D_p + D_f \tag{37}$$

where D_p and D_f represent the pressure and friction drag, respectively, with [26]

$$D_p = \sum_{i=1}^{N_a} 2\gamma p_\infty M\left[\alpha_o + \alpha_i + \left(\frac{T}{C}\right)^2\right]\frac{Cl}{N_a} \tag{38}$$

and

$$D_f = \sum_{i=1}^{N_a}\left[\frac{2l}{N_a}\int_{-\frac{c}{2}}^{\frac{c}{2}} T_f'(x)\cos(\alpha_o + \alpha_i)\,\mathrm{d}x\right] \tag{39}$$

In Eqs. (38) and (39), p_∞ is the atmospheric pressure, γ the ratio of specific heats, M the flight Mach number, N_a the number of segments into which the airfoil is divided for numerical computations, and T_f' the shear stress, which can be determined from the flight conditions.

In the second example, shown in Fig. 5, both the structural weight of the supersonic wing and the energy required for a specific flight condition are minimized and the flutter velocity is maximized. The finite element method is used for structural idealization. The thicknesses of the skin, the thickness of the ribs and spars, and the cross-sectional areas of the pin-jointed bars are treated as design variables. The gust stress is constrained by an upper bound and the design variables are restricted to lie between specified limits. Thus the optimization problem can be stated as follows: Find $\mathbf{X} = \{x_1, x_2, \ldots, x_6\}$ which minimizes $f_1(\mathbf{X})$, and $f_2(\mathbf{X})$ and maximizes $f_3(\mathbf{X})$ subject to

$$\sigma_g(\mathbf{X}) \le \sigma_g^{(u)} \tag{40}$$

$$x_i^{(l)} \le x_i \le x_i^{(u)} \qquad i = 1, 2, \ldots, 6 \tag{41}$$

Here the structural weight is given by

$$f_1(\mathbf{X}) = \sum_{i=1}^{N_s} \rho t_{si} A_{si} + \sum_{i=1}^{N_w} \rho t_{wi} A_{wi} + \sum_{i=1}^{N_b} \rho l_{bi} A_{bi} \tag{42}$$

and $f_2(\mathbf{X})$ is given by Eq. (36) with the total drag D composed of pressure drag D_p and friction drag D_f:

$$D_p = 2M_\infty^2 P_\infty \iint_{SA}\left[(\alpha_0 - w_x)^2 + d_x^2 - \frac{1}{4}\gamma(1+\gamma)M_\infty^2(6\alpha_0 d_x w_x - 3 d_x w_x)\right]\mathrm{d}x\,\mathrm{d}y \tag{43}$$

$$D_f = \iint_{SA}\left[\tau_{Fl}\cos\left(\alpha_o - \frac{\partial w}{\partial x} + \frac{\partial d}{\partial x}\right) + \tau_{Fu}\cos\left(\alpha_o - \frac{\partial w}{\partial x} - \frac{\partial d}{\partial x}\right)\right]\mathrm{d}x\,\mathrm{d}y \tag{44}$$

where τ_{Fl} and τ_{Fu} are the skin friction stress at the lower and upper surfaces of the wing, respectively, and SA is the aerodynamic field. The flutter Mach number, $f_3(\mathbf{X})$, can be calculated as described in the Appendix.

Table 1 Design data for example wing 1

Material properties (titanium) of wing:	
Young's modulus	109.97 GPa
Shear modulus	43.988 GPa
Material density	4500 kg/m^3
Additional masses:	
Fuselage weight	126.95 kg
Engine weight	63.45 kg
Fuel weight	105.38 kg
Static load condition:	
Altitude	10,668 m
Air pressure	23,844.4 Pa
Speed of sound	296.6 m/s
Air density	0.379 kg/m^3
Steady-state flight Mach no.	2.0
Pull-up acceleration	2.0 g
Flight duration	1 h
Semispan	9.0 m
Solidity ratio of the cross section	0.075
Gust load condition:	
Discrete gust (cosine type):	
Maximum vertical velocity	3.0 m/s
Length of gust	10 chords
Forward velocity of flight	154.8384 m/s
Altitude	7620 m
Air density	0.5494 kg/m^3
Power spectral approach:	
Scale of turbulence	762 m

Solution Procedure

A large number of methods have been developed for the solution of multi-objective optimization problems. The game theory approach is expected to yield more rational compromise solutions to multi-objective design problems. In this approach, each objective is associated with a player competing to optimize his/her standing in a system subjected to limited resources. Two theories have been used to describe the interaction of the players: the noncooperative theory, based on the concept of Nash equilibrium, and the cooperative theory, based on the concept of the Pareto minimum solution. This work uses the concept of a cooperative game in which each player competes to optimize his/her standing in a system subject to limited resources while willing to cooperate with other players. Here, each player is a member of a team willing to compromise his own objective to improve the solution as a whole. The team allocates the resources with the intent that all players should be able to achieve their objectives as optimal as possible—in other words, a Pareto optimal solution. The procedure of finding an optimal compromise solution according to the original cooperative game theory has been inefficient and requires much manual effort for the designer [10]. In this paper, to increase the efficiency, the original game theory method has been modified such that the Pareto optimal solution generation and the maximization of the supercriterion is performed simultaneously [11]. To find a compromise solution for each of the individual objective functions, which achieves a value that is as far as possible from the respective worst value, the following procedure is adopted:

1) Start from an initial design vector $\mathbf{X}_0$ and minimize each objective function $f_i(\mathbf{X})$, $i = 1, 2, \ldots, k$ subject to the stated constraints. For the solution of the single-objective multivariable constrained optimization problems, nonlinear programming

Table 2 Design data for example wing 2

Material properties:	Material	Aluminum
	Young's modulus	68.95 GPa
	Poisson's ratio	0.333
	Density	2768 kg/m^3
Details of the weight:	Planform area	136.99 m^2
	Engines	5669 kg
	Fuselage and payload	32,658.6 kg
	Fuel	41,957.9 kg
	Maximum takeoff mass	174,632.9 kg
Flight conditions data:		
Altitude	7620 m	
Pull-up acceleration	3.75 g	
Flight Mach no.	1.89	
Pressure of air	37,649.7 Pa	
Density of air	0.5498 kg/m^3	
Gust analysis data:		
Discrete gust, cosine type	Maximum vertical velocity = 1.5233 m/s	
Length of gust = 5 chords	Forward velocity of flight = 154.84 m/s	
Altitude = 7620 m		
For spectrum approach	Scale of turbulence = 7620 m	

Table 3 Probabilistic optimization results for double-wedge airfoil

	Initial design	Bounds Lower	Upper	Optimum design
Design variables				
x_1, mm	41.0	17.8	266.0	42.10
x_2, mm	476.0	50.0	652.0	475.62
c_1	0.333	0.0	1.0	0.0110
c_2	0.333	0.0	1.0	0.0766
Behavior constraint				
Gust stress				
σ_g, MPa	22.22[a]		22.62	16.28

$$P = \begin{bmatrix} f_1(x) & f_2(x) & f_3(x) \\ 410.56 & 131.7 & -6.5370 \\ 426.33 & 95.34 & -6.6952 \\ 421.15 & 146.53 & -9.5357 \end{bmatrix}$$

Multi-objective optimization results

Objective functions	Min	Max	MOO
Structural weight of airfoil, kg	410.56	426.324	421.62
Energy, GJ	95.34	146.53	119.35
Negative flutter Mach no. M_F	−9.5357	−6.5370	−7.5722
In multi-objective optimization (MOO)			
No. of functions evaluation = 11			
No. of gradient evaluation = 10			

[a]Active constraint.

techniques (penalty function approach and sequential quadratic programming) are used. Then construct a matrix [P] as

$$[P] = \begin{bmatrix} f_1(X_1^*) & f_2(X_1^*) & \cdots & f_k(X_1^*) \\ f_1(X_2^*) & f_2(X_2^*) & \cdots & f_k(X_2^*) \\ \vdots & \vdots & \vdots & \vdots \\ f_1(X_k^*) & f_2(X_k^*) & \dots & f_k(X_k^*) \end{bmatrix}$$

It can be seen that the diagonal elements in the matrix [P] are the minima in their respective columns.

2) Formulate a suitable bargaining model or supercriterion, S, as

$$S = \prod_{i=1}^{k} \{ f_{ni}^{\max} - f_{ni}(\mathbf{X}_i^*) \} \tag{45}$$

where f_{ni} denotes the normalized ith objective function:

$$f_{ni} = \frac{f_i^{\max} - f_i(\mathbf{X})}{f_i^{\max} - f_i^*}$$

3) Formulate a suitable Pareto optimal objective function, F_c as

Table 4 Probabilistic optimization results for wing (example 2)

	Initial Design	Bounds Lower	Upper	Optimum design
Design variables				
x_1, mm	3.81	1.016	12.70	10.97
x_2, mm	3.81	1.016	12.70	4.410
x_3, mm	3.81	1.016	12.70	3.270
x_4, mm	3.81	1.016	12.70	3.332
x_5, mm	3.81	1.016	12.70	2.210
x_6, mm^2	161.29	25.81	322.58	194.77
c_1	0.333	0.00	1.0	0.0422
c_2	0.333	0.00	1.0	0.0400
Behavior constraint				
Gust stress				
σ_g, MPa	130.38		304.72	275.76[a]

$$P = \begin{bmatrix} f_1(x) & f_2(x) & f_3(x) \\ 3643.26 & 1837.21 & -5.2974 \\ 4813.15 & 1797.13 & -5.0093 \\ 10,189.22 & 1953.20 & -5.6723 \end{bmatrix}$$

Multi-objective optimization results

Objective functions	Min	Max	MOO
Structural weight of airfoil, kg	3643.26	10,189.22	5481.30
Energy, GJ	1797.11	1953.23	1909.10
Negative flutter Mach no. M_F	−5.6723	−5.0093	−5.1110
In multi-objective optimization (MOO)			
No. of functions evaluation = 31			
No. of gradient evaluation = 7			

[a]Active constraint.

Table 5 Interval optimization results for double-wedge airfoil

	Initial design	Bounds: Lower	Bounds: Upper	Optimum design
Design variables				
x_1, mm	[40.6 42.0]	[17.8 13.0]	[240 330]	[34.3 45.3]
x_2, mm	[475 477]	[49.7 63.5]	[500 534]	[475.0 477.0]
c_1	0.333	0.0	1.0	[0.040 0.070]
c_2	0.333	0.0	1.0	[0.041 0.068]
Behavior constraint				
Gust stress				
σ_g, MPa	[20.597 22.32][a]		22.34	[18.724 20.63][a]

$$P = \begin{bmatrix} f_1(x) & f_2(x) & f_3(x) \\ [401.345 \quad 416.65] & [100.3 \quad 173.0] & [-7.7356 \quad -3.3158] \\ [390.276 \quad 418.07] & [78.92 \quad 113.0] & [-7.2633 - 4.2109] \\ [425.673 \quad 425.93] & [110.11 \quad 119.31] & [-9.9230 \quad -9.2833] \end{bmatrix}$$

Multi-objective optimization results

Objective functions	Min	Max	MOO
Structural weight, kg	[401.345 416.65]	[425.67 425.93]	[396.07 424.20]
Energy, GJ	[78.92 113.0]	[100.3 173.01]	[110.11 121.3]
Negative flutter Mach no. M_F	[−9.9923 −9.2833]	[−7.2633 −4.2109]	[−8.8595 −5.5996]

In multi-objective optimization (MOO)
No. of functions evaluation = 11
No. of gradient evaluation = 10

[a]Active constraint.

minimize

$$F_c(\mathbf{c}, \mathbf{X}) = \sum_{i=1}^{k-1} c_i f_i(\mathbf{X}) + \left(1 - \sum_{i=1}^{k-1} c_i\right) f_k(\mathbf{X}) \tag{46}$$

subject to

$$c_i \geq 0, \qquad i = 1, 2, \ldots, k-1 \tag{47}$$

and

$$\sum_{i=1}^{k} c_i = 1 \tag{48}$$

where $\mathbf{c} = (c_1, c_2, \ldots, c_k)^T$ denotes the vector of constants or weights indicating the relative importance of the various objective functions for minimization.

4) Construct a new (composite) objective ($\text{OBJ} = F_c - S$) using the supercriterion (S) and the Pareto optimal objective function (F_c) defined by Eqs. (45) and (46).

Table 6 Interval optimization results for wing (example 2)

	Initial design	Bounds: Lower	Bounds: Upper	Optimum design
Design variables				
x_1, mm	[3.81 3.82]	1.016	12.70	[9.085 19.64]
x_2, mm	[3.81 3.82]	1.016	22.86	[16.74 21.92]
x_3, mm	[3.81 3.82]	1.016	12.70	[2.33 2.80]
x_4, mm	[3.81 3.82]	1.016	22.86	[13.34 20.53]
x_5, mm	[3.81 3.82]	1.016	22.86	[4.29 4.87]
x_6, mm^2	[161.16 161.35]	25.8	322.58	[67.48 94.45]
c_1		0.0	1.0	[0.0575 0.0781]
c_2		0.0	1.0	[0.5738 0.7698]
Behavior constraint				
Gust stress				
σ_g, MPa	[126.45 131.76]		275.76	[248.8 268.245][a]

$$P = \begin{bmatrix} f_1(x) & f_2(x) & f_3(x) \\ [3307.19 \quad 3629.25] & [1792.9 \quad 1916.9] & [-5.2182 \quad -3.5503] \\ [6799.5 \quad 8147.11] & [1793.2 \quad 1798.0] & [-6.2997 \quad -5.9970] \\ [8940.5 \quad 10,205.5] & [1900.2 \quad 2117.7] & [-7.8240 \quad -6.1403] \end{bmatrix}$$

Multi-objective optimization results

Objective functions	Min	Max	MOO
Structural weight, kg	[3307.19 3629.25]	[8940.5 10,205.5]	[3753.99 3764.43]
Energy, GJ	[1793.2 1798.0]	[1900.2 2117.7]	[1762.9 1834.0]
Negative flutter Mach no. M_F	[−7.8240 −6.1403]	[−5.2182 −3.5503]	[−7.7003 −5.9854]

In multi-objective optimization (MOO)
No. of functions evaluation = 37
No. of gradient evaluation = 19

[a]Active constraint.

Table 7 Deterministic optimization results for double-wedge airfoil

	Initial design	Bounds Lower	Bounds Upper	Optimum design
Design variables				
x_1, mm	41.0	17.8	266.0	41.1
x_2, mm	476.0	50.0	652.0	476.2
c_1	0.333	0.0	1.0	0.0420
c_2	0.333	0.0	1.0	0.0500
Behavior constraint				
Gust stress, σ_g, MPa	22.21[a]		22.34	20.57[a]

$$P = \begin{bmatrix} f_1(x) & f_2(x) & f_3(x) \\ 404.53 & 114.57 & -4.5018 \\ 419.38 & 92.83 & -5.7351 \\ 412.37 & 150.40 & -9.7607 \end{bmatrix}$$

Multi-objective optimization results

Objective functions	Min	Max	MOO
Structural weight of airfoil, kg	404.53	419.39	418.43
Energy, GJ	92.83	150.40	117.11
Negative flutter Mach no. M_F	−9.761	−4.502	−7.8894
In multiobjective optimization (MOO)			
No. of functions evaluation = 21			
No. of gradient evaluation = 10			

[a]Active constraint.

5) Solve the following problem:

Find $\mathbf{Y}^*$ which minimizes OBJ subject to the constraints in Eqs. (40) and (41) and

$$f_{ni}^{\min} \leq f_{ni}(\mathbf{x}) \leq f_{ni}^{\max}, \qquad i = 1, 2, \ldots, k \tag{49}$$

$f_i^{\min}$ is the minimum and $f_i^{\max}$ is the maximum value in the ith row of matrix $[P]$. The design vector $\mathbf{Y}$ now includes not only the original design vector $\mathbf{X}$ but also the weights or constants associated with the Pareto optimal objective function.

6) Find the optimal compromise solution of the original multi-objective optimization problem from the solution found in step 5.

Because all the system parameters, including the design variables and the objective functions, are treated as interval variables, the elements of the matrix $[P]$ will be interval numbers. So we need to apply interval arithmetic to every step of the calculations. During actual computation, we need to adjust the order in which different interval parameters are considered in any specific equation. This is because, when the program executes the equation using interval parameters, the new order will not only minimize the computational time but also lead to a reduced interval range for the result. It has been observed that the widths (intervals) of the response parameters predicted become wider than the true widths with an increase in the size of the problem. To avoid the unnecessary growth of the intervals of the response parameters, an interval-truncation method described

Table 8 Deterministic optimization results for wing (example 2)

	Initial design	Bounds Lower	Bounds Upper	Optimum design
Design variables				
x_1, mm	3.81	1.016	12.70	11.76
x_2, mm	3.81	1.016	22.86	20.96
x_3, mm	3.81	1.016	12.70	2.370
x_4, mm	3.81	1.016	22.86	18.86
x_5, mm	6.35	1.016	12.70	4.550
x_6, mm^2	161.29	25.81	322.58	89.74
c_1	0.333	0.0	1.0	0.0699
c_2	0.333	0.0	1.0	0.7003
Behavior constraint				
Gust stress σ_g, MPa	130.386		275.8	260.1[a]

$$P = \begin{bmatrix} f_1(x) & f_2(x) & f_3(x) \\ 3472.3 & 1854.6 & -4.0503 \\ 6852.1 & 1795.0 & -6.0033 \\ 10,929.0 & 2017.2 & -6.9454 \end{bmatrix}$$

Multi-objective optimization results

Objective functions	Min	Max	MOO
Structural weight of airfoil, kg	3472.30	10,929.0	3756.76
Energy, GJ	1795.0	2017.2	1800.9
Negative flutter Mach no. M_F	−6.9454	−4.0503	−6.3273
In multi-objective optimization (MOO)			
No. of functions evaluation = 41			
No. of gradient evaluation = 13			

[a]Active constraint.

earlier is used. The purpose of truncation is to make reasonable modification to the output parameters based on the ranges of the input parameters before applying it for the next step of operations.

In some computational steps, the use of interval arithmetic may lead to a result that is in conflict with the physics of the problem. If these invalid operations are used in the computation, the final solution will not be correct. In those cases, it is safe to apply the combinatorial method instead of the interval operation in order to comply with the physical logic. It is to be noted that the optimization method is found to converge to the correct solution as long as the ranges of the input interval parameters are small and the ranges of the response parameters are restricted to not grow unnecessarily.

Numerical Results and Discussion

The optimization of two example wings is considered for illustration. The first example, shown in Fig. 4, is assumed to be made of titanium. The thickness T and the chord length C are the design variables. The design data for the optimization of this hollow symmetric double-wedge airfoil are given in Table 1. The second example deals with the design of the wing structure shown in Fig. 5. The pertinent data for this example wing are given in Table 2. The flight condition, indicated in Table 1, is considered for this wing as well.

For the interval analysis, each input parameter described in Table 1 is represented as a range using the interval $(x - \Delta x, x + \Delta x)$ where x is the mean, deterministic, or nominal value of the parameter and Δx is the deviation from the mean value, taken as $0.05x$. For comparison purposes, the optimum design of the wing is also found using a probabilistic analysis. The probabilistic analysis is performed by representing each uncertain parameter as a random variable following normal distribution with a known mean value x and standard deviation σ_x which is taken as one-third of Δx. By computing the mean value and standard deviations of the outputs from the mean value and standard deviations of the uncertain input parameters using the partial derivative rule, the constraints for the probabilistic optimization are considered as [28]

$$\bar{g} + 3S_g \leq g_{\text{limit}} \tag{50}$$

where $\bar{g}$ is the mean value, S_g is the standard deviation, and g_{limit} is the allowable limit for each constraint. The mean $\bar{g}$ and the standard deviation S_g are computed using the partial derivative rule, based on a first-order Taylor's series expansion of the function $g(\mathbf{Y})$ about the mean values of the unknown parameters y_i of the unknown vector $\mathbf{Y}$.

In both the wing examples, piston theory is used to calculate the aerodynamic drag. A computer program is developed for finding the solutions of interval optimization problems. The optimum values of the weight, energy, and flutter Mach number for examples 1 and 2 corresponding to a fixed set of constraint values $\alpha_g^{(u)}$ are obtained. For comparison, the results obtained by considering all the constraints and the objective functions to be probabilistic are reported in Tables 3 and 4. For interval analysis the problem is solved by treating all the design parameters as interval numbers. The initial and optimum interval analysis-based designs, shown in Tables 5 and 6 are found to be closer to the solutions obtained using a deterministic analysis (Tables 7 and 8). All the results indicate that the optimum solution obtained with the interval analysis is in good agreement with the one obtained using a deterministic and probabilistic analysis (for comparable data).

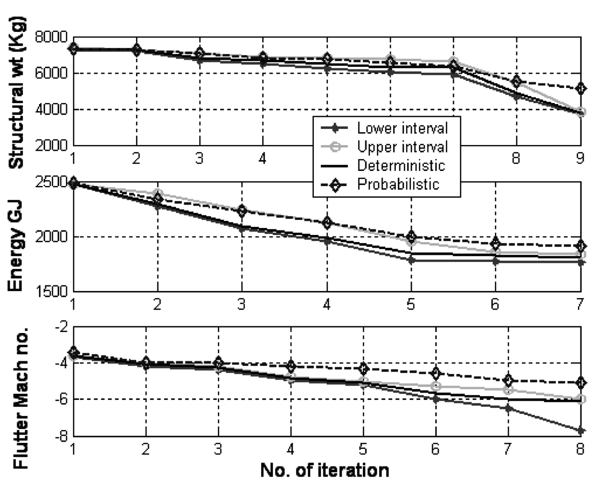

Fig. 6 Multi-objective optimization of example wing 2 under gust loads in progress, deterministic, probabilistic, and interval analyses.

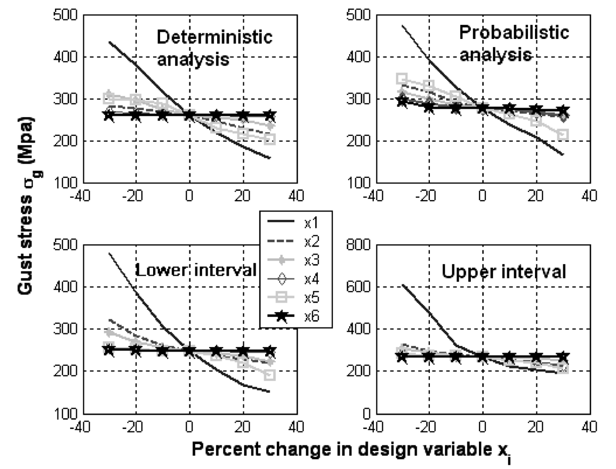

Fig. 7 Sensitivity of gust stress to design variables for example wing 2, with deterministic, probabilistic, and interval analyses.

Figure 6 shows the progress of multi-objective optimization or Pareto optimal solutions with the number of iterations for the designs based on all three types of analyses. A sensitivity analysis is performed on the optimization results of example wing 2. Figure 7 shows the sensitivity of the gust-induced stress with the percent changes in the values of design variables. The optimum design is taken as the reference design and the value of each of the design variables is changed by $\pm 30\%$ in steps of 10%. For all three types of analysis, it is found that the maximum gust stresses are most sensitive to the variation of skin thickness near the root of the wing. These results are expected to be useful when the designer is interested in altering the optimum design variables to satisfy any potential new design requirements.

Conclusions

A methodology is presented for the interval analysis-based multicriteria optimum design of airplane wing structures under dynamic conditions, including gust loads. The method uses a modified cooperative game theory approach. The optimum design procedure is demonstrated through the designs of a hollow symmetric double-wedge airfoil and a supersonic transport wing. Three objectives, namely, the minimizations of structural weight and energy and maximization of flutter Mach number during a specified flight condition are considered in the problem formulation. The aim of the work is to determine an optimal tradeoff (Pareto optimal solution) between the three objectives based on a specified supercriterion. The results obtained with the interval analysis-based approach are found to be in good agreement with the one obtained using a deterministic analysis for comparable data. Because of the random natures of the forward velocity and vertical velocity of gust, a probabilistic approach is also used and the resulting optimization results are compared with those obtained using deterministic and interval analyses. Because the actual values of the gust loads or their probability distributions cannot be predicted precisely, the interval analysis is expected to be more realistic and, hence, should be used for the optimum design of airplane wing structures.

Appendix: Flutter Analysis

For the steady state, oscillations of the system in a state of neutral stability may be expressed [in terms of the generalized coordinates $\xi_i(t)$] as

$$[[K]_{s\times s} - \omega^2[M]_{s\times s} + [Q]_{s\times s}]\boldsymbol{\xi}_{s\times 1} = \mathbf{0}_{s\times 1} \quad (A1)$$

where the $[K]$ and $[M]$ are the stiffness and mass matrices, respectively. The aerodynamic matrix, according to the piston theory, is given by

$$[Q^{(i)}] = 2\rho_\infty a_\infty V_\infty[A^{(i)}] + 2i\rho_\infty a_\infty w[B^{(i)}] + \rho_\infty(\gamma+1)V_\infty^2[C^{(i)}] + i\rho_\infty(\gamma+1)V_\infty\omega[D^{(i)}] \quad (A2)$$

where the elements of the matrices $[A]$ to $[D]$ are given by

$$[A^{(i)}] = \iint \mathbf{a}^T \frac{\partial \mathbf{a}}{\partial x}\,\mathrm{d}x\,\mathrm{d}y \quad (A3)$$

$$[B^{(i)}] = \iint \mathbf{a}^T \mathbf{a}\,\mathrm{d}x\,\mathrm{d}y \quad (A4)$$

$$[C^{(i)}] = \iint \frac{\partial Z}{\partial x}\mathbf{a}^T \frac{\partial \mathbf{a}}{\partial x}\,\mathrm{d}x\,\mathrm{d}y \quad (A5)$$

$$[D^{(i)}] = \iint \frac{\partial Z}{\partial x}\mathbf{a}^T \mathbf{a}\,\mathrm{d}x\,\mathrm{d}y \quad (A6)$$

The double integrals of Eqs. (A3–A6) are to be evaluated over the planform area of the ith element. The requirement for a nontrivial solution to Eq. (A1) is that the determinant of the coefficient matrix of $\boldsymbol{\xi}$ must vanish. Thus the flutter equation becomes

$$|[K] - \omega^2[M] + [Q]| = 0 \quad (A7)$$

From Eq. (A2), it can be seen that the elements of $[Q]$ are complex functions of the freestream velocity V_∞, oscillation frequency ω, density of air ρ_∞, and freestream speed of sound a_∞. For any given atmospheric conditions ρ_∞ and a_∞, Eq. (A7) represents a complex, nonlinear, double eigenvalue problem because there are two unknowns V_∞ and ω.

Equation (A7) can be written in a more convenient form as

$$\left|\frac{V}{a_\infty}\frac{1}{2\rho_\infty}[M_{ii}\{X(\omega_i/\omega_1)^2 - 1\}] + (b_r/k_r)^2\left([\mathrm{A}] + \frac{\gamma+1}{2}\frac{V}{a_\infty}[\mathrm{C}]\right) + i(b_r/k_r)\left([B] + \frac{\gamma+1}{2}\frac{V}{a_\infty}[D]\right)\right| = 0 \quad (A8)$$

with $X = (\omega_1/\omega)^2$, $k_r = (b_r \cdot \omega/V) =$ reduced frequency, and $b_r =$ some reference length. The formulation of Eq. (A8) is more convenient, compared to Eq. (A7), to solve the flutter problem with Mach number (V/a_∞) and the reduced-frequency (k_r) as the unknowns. In the present work, Eq. (A8) is solved by a double iterative process, also known as the $V - g$ method. The lowest freestream velocity and the corresponding frequency obtained by solving Eqs. (A7) or (A8) will be, respectively, the flutter velocity V_F and the flutter frequency ω_F.

References

[1] Kuhn, H. W., and Tucker, A. W., "Nonlinear Programming," *Proceedings of the Second Berkeley Symposium on Mathematical Statistics and Probability*, edited by J. Neyman, J., Univ. of California, Berkeley, CA, 1951, pp. 481–491.

[2] Rao, S. S., Pan, T. S., and Venkayya, V. B., "Robustness Improvement of Actively Controlled Structures Through Structural Modifications," *AIAA Journal*, Vol. 28, No. 2, 1990, pp. 353–361. doi:10.2514/3.10396

[3] Rao, S. S., Venkayya, V. B., and Khot, N. S., "Game Theory Approach for the Integrated Design of Structures and Controls," *AIAA Journal*, Vol. 26, No. 4, 1988, pp. 463–469. doi:10.2514/3.9916

[4] Osman, M. S., Abo-Sinna, M. A, Amer, A. H., and Emam, O. E., "A Multi-Level Nonlinear Multi-Objective Decision Making Under Fuzziness," *Applied Mathematics and Computation*, Vol. 153, 2004, pp. 239–252. doi:10.1016/S0096-3003(03)00628-3

[5] Rao, S. S., "Game Theory Approach for Multiobjective Structural Optimization," *Computers and Structures*, Vol. 25, No. 1, 1987, pp. 119–127. doi:10.1016/0045-7949(87)90223-9

[6] Rao, S. S., Sundararaju, K., Prakash, B. G., and Balakrishna, C., "Multi-Objective Fuzzy Optimization Techniques for Engineering Design," *Computers and Structures*, Vol. 42, No. 1, 1992, pp. 37–44. doi:10.1016/0045-7949(92)90534-7

[7] Yu, M., and Xu, C., "Multi-Objective Fuzzy Optimization of Structures Based on Generalized Fuzzy Decision-Making," *Computers and Structures*, Vol. 53, No. 2, 1994, pp. 411–417. doi:10.1016/0045-7949(94)90213-5

[8] Rao, S. S., and Hati, S. K., "Game Theory Approach in Multicriteria Optimization of Function Generating Mechanisms," *Journal of Mechanical Design*, Vol. 101, 1979, pp. 398–406.

[9] Vincent, T. L., "Game Theory as a Design Tool," *Transactions of the ASME. Journal of Mechanisms, Transmissions, and Automation in Design*, Vol. 105, No. 1, 1983, pp. 165–170.

[10] Rao, S. S., "Game Theory Approach for Multiobjective Structural Optimization," *Computers and Structures*, Vol. 25, No. 1, 1987, pp. 119–127. doi:10.1016/0045-7949(87)90223-9

[11] Rao, S. S., and Freiheit, T. I., "A Modified Game Theory Approach to Multiobjective Optimization," *Transactions of the ASME*, Vol. 113, 1991, pp. 286–291. doi:10.1115/1.2912781

[12] Dhingra, A. K., and Rao, S. S., "A Cooperative Fuzzy Game Theoretic Approach to Multiple Objective Design Optimization," *European Journal of Operational Research*, Vol. 83, No. 3, 1995, pp. 547–567.

[13] Rao, S. S., and Berke, L., "Analysis of Uncertain Structural Systems Using Interval Analysis," *AIAA Journal*, Vol. 35, No. 4, 1997, pp. 727–735. doi:10.2514/2.164

[14] Dessombz, O., Thouverez, F., Laine, J. P., and Jezequel, L., "Analysis of Mechanical Systems Using Interval Computations Applied to Finite Element Methods," *Journal of Sound and Vibration*, Vol. 239, No. 5, 2001, pp. 949–968. doi:10.1006/jsvi.2000.3191

[15] Philip, D., "Summary of Information Relating to Gust Loads on Airplanes," NACA Rept. 997, 1950.

[16] Clementson, G. C., "An Investigation of the Power Spectral Density of Atmospheric Turbulence," Ph.D. Thesis, MIT, Cambridge, MA, 1950.

[17] Rao, S. S., "Optimization of Airplane Wing Structures Under Gust Loads," *Computers and Structures*, Vol. 21, No. 4, 1985, pp. 741–749. doi:10.1016/0045-7949(85)90150-6

[18] Rao, S. S., "Automated Optimum Design of Wing Structures: A Probabilistic Approach," *Computers and Structures*, Vol. 24, No. 5, 1986, pp. 799–808. doi:10.1016/0045-7949(86)90145-8

[19] Perry, B. III, Pototzky, A. S., and Wood, J. A., "NASA Investigation of a Claimed Overlap Between Two Gust Response Analysis Method," *Journal of Aircraft*, Vol. 27, No. 7, 1990, pp. 605–611. doi:10.2514/3.25329

[20] Yang, J. S., Nikolaidis, E., and Haftka, R. T., "Design of Aircraft Wings Subjected to Gust Loads: A System Reliability Approach," *Computers and Structures*, Vol. 36, No. 6, 1990, pp. 1057–1066. doi:10.1016/0045-7949(90)90213-L

[21] Rao, S. S., and Chen, L. I., "Numerical Solution of Fuzzy Linear Equations in Engineering Analysis," *International Journal for Numerical Methods in Engineering*, Vol. 43, 1998, pp. 391–408. doi:10.1002/(SICI)1097-0207(19981015)43:3<391::AID-NME417>3.0.CO;2-J

[22] Tang, D., and Dowell, E. H., "Experimental and Theoretical Study of Gust Response for High-Aspect-Ratio Wing," *AIAA Journal*, Vol. 40, No. 3, 2002, pp. 419–429. doi:10.2514/2.1691

[23] Pettit, C. L., Grandhi, R. V., "Optimization of a Wing Structure for Gust Response and Aileron Effectiveness," *Journal of Aircraft*, Vol. 40, No. 6, 2003, pp. 1185–1191. doi:10.2514/2.7208

[24] Kim, T. U., and Hwang, I. H., "Optimal Design of Composite Wing Subjected to Gust Loads," *Computers and Structures*, Vol. 83, 2005, pp. 1546–1554. doi:10.1016/j.compstruc.2005.02.002

[25] Houolt, J. C., and Kordes, E. E., "Structural Response to Discrete and Continuous Gusts of an Airplane Having Wing Bending Flexibility and a Correlation of Calculated and Flight Results," NACA Rept. 1181, 1954.

[26] Majumder, L., "An Interval Analysis-Based Multiobjective Optimization of Supersonic Wing Structures," Ph.D. Thesis, University of Miami, Coral Gables, FL, Aug. 2007.

[27] Schmit, L. A., and Thronton, W. A., "Synthesis of an Airfoil at Supersonic Mach Number," NASA Rept. CR-144, 1965.

[28] Rao, S. S., *Reliability-Based Design*, McGraw–Hill, New York, 1992.

E. Livne
Associate Editor